Effects of vanadium content on the carbides transformation and strengthening mechanism of MPS700V hot-work die steel at room and elevated temperatures

Zhang, Zunjun; Zhang, Jishan; Lian, Yong; Ma, Minyu; Zhao, Chao; Ye, Huanyu; Li, Gaojie; Zhang, Cheng; Huang, Jinfeng

DOI
10.1016/j.msea.2021.141091

Publication date
2021

Document Version
Final published version

Published in
Materials Science and Engineering A

Citation (APA)
Zhang, Z., Zhang, J., Lian, Y., Ma, M., Zhao, C., Ye, H., Li, G., Zhang, C., & Huang, J. (2021). Effects of vanadium content on the carbides transformation and strengthening mechanism of MPS700V hot-work die steel at room and elevated temperatures. *Materials Science and Engineering A*, *813*, Article 141091. https://doi.org/10.1016/j.msea.2021.141091

Materials Science & Engineering A 813 (2021) 141091

Contents lists available at ScienceDirect

Materials Science & Engineering A

journal homepage: http://www.elsevier.com/locate/msea

Effects of vanadium content on the carbides transformation and strengthening mechanism of MPS700V hot-work die steel at room and elevated temperatures

Zunjun Zhang [a], Jishan Zhang [a], Yong Lian [b], Minyu Ma [b], Chao Zhao [b], Huanyu Ye [c], Gaojie Li [d], Cheng Zhang [a,**], Jinfeng Huang [a,*]

[a] State Key Laboratory for Advanced Metals and Materials, University of Science and Technology Beijing, No. 30, Xueyuan Road, Beijing 100083, China
[b] Institute for Advanced Materials and Technology, University of Science and Technology Beijing, No. 30, Xueyuan Road, Beijing 100083, China
[c] School of Mathematics and Physics, University of Science and Technology Beijing, No. 30, Xueyuan Road, Beijing 100083, China
[d] Mechanical Maritime and Material Engineering, Delft University of Technology, Mekelweg 4, 2628 CD Delft, Netherlands

ARTICLE INFO

Keywords:
Hot-work die steel
Nano-carbides
Vanadium content
Strengthening mechanism
High-temperature strength

ABSTRACT

The effects of vanadium content on the microstructural and mechanical properties of a newly developed hot-work die steel (MPS700V) at room and elevated temperatures have been investigated in this paper. It shows that the ultimate tensile strength (UTS) of MPS700V at room temperature and 700 °C are both strongly dependent on the V content. With the increase of V content from 0 to 1.2% V, The UTS at room temperature increases from 1127 MPa to 1442 MPa, and the UTS at 700 °C increases from 400 MPa to 550 MPa. The transmission electron microscope (TEM) shows that the addition of V is beneficial to increase the nucleation rate and volume fraction of MC nano-carbides during the tempering process, and the size of the MC nano-carbides decreases with the increase of V content. The addition of V also increases the thermal stability of MC nano-carbides at 700 °C, which can be related to the reducing the interface mismatch between MC and matrix. Furthermore, a transformation from Orowan bypass strengthening mechanism to shearing strengthening mechanism caused by the V addition is proposed based on the theoretical analysis and TEM observation.

1. Introduction

Hot-work die steels are widely used in the hot-working molds of industrial parts prepared by hot forging, hot extrusion and die casting [1–3]. They need to endure rapid heating and cooling impact in addition to the heavy mechanical load when directly interacting with hot metals. Their service temperature during the hot forging, hot extrusion and die casting process can reach to more than 500–600 °C (local temperature can reach almost 700 °C [4,5]). Therefore a high strength at elevated temperature is necessary for the hot-work die steel. However, for many hot-work die steels, their strength decreased rapidly at the temperature exceeding 600 °C, for example, the ultimate strength of widely used H13 steel decreases from more than 1700 MPa to about 600 MPa at the temperature of 640 °C, and even less than 300 MPa at 700 °C, which greatly shorten the service life [1,5–9]. Therefore, with the increasing demands of service temperature and lifetime of hot-work dies, the hot-work die steels with higher thermal stability and higher temperature strength become more and more attractive.

Typical microstructure of hot-work die steels containing carbide forming elements as Cr, Mo and V. Extensive studies have been carried out to explore the effects of alloying elements on the precipitation of secondary carbides [10–14]. Chromium (Cr) is generally considered to be an alloying element that is not beneficial to the high temperature strength of the material because it is easy to form carbides with large volume and insufficient thermal stability [7,15,16]. However, some studies [17–19] have shown that Cr can participate in the precipitation of nano-scale MC carbides and M_2C carbide to provide strengthening effect as well as improve the thermal stability of sub-grain and grain boundaries. Molybdenum (Mo) can not only reinforce steel strength at room temperature by promoting the precipitation of fine M_2C carbides, but also enhance steel high-temperature yield strength through improving carbide stability at high temperature [10–13]. The addition

* Corresponding author.
** Corresponding author.
E-mail addresses: zhangcheng@ustb.edu.cn (C. Zhang), ustbhuangjf@163.com (J. Huang).

https://doi.org/10.1016/j.msea.2021.141091
Received 14 January 2021; Received in revised form 8 March 2021; Accepted 9 March 2021
Available online 13 March 2021

of a small amount of vanadium (V) typically of 0.1–0.2 wt% or less in steel materials can effectively increase the room temperature strength by 70–200 MPa [20–23]. V and niobium (Nb) are also the major constituent elements of MC nano-carbides [16,21,24–26], which can improve the thermal stability of nano-carbides as well as the stability of microstructures and high temperature properties. More precipitation of carbides by increasing the content of alloying elements and carbon is considered as an effective strategy to reinforce the high-temperature strength of steels [25–29]. However, the excessive addition of carbide-forming elements leads to the coarsen of carbides, which contributes little to the high-temperature strength but also results in the room-temperature brittleness of the steels [30]. Therefore, the optimal range of alloying elements is important for the performance of hot-work die steel.

In the previous work, a newly developed hot-work die steel (MPS700V) strengthened by nano-carbides with high thermal stability was reported [31], whereas the role of alloy elements, especially V, in the precipitation of nano-carbides and the strengthening mechanism is still not well understood. Therefore, in this paper the influence of V content on the mechanical properties and microstructure evolution, especially the precipitation of nano-carbides in the MPS700V steel are investigated in detail.

2. Materials and methods

The nominal chemical compositions (wt. %) of the test alloy samples are listed in Table 1. To investigate the effects of V on the mechanical properties and high temperature strength, the test alloys were designed with different V contents and prepared by vacuum induction melting. Besides, homogenization at 1280 °C for 10 h and furnace-cooling were also conducted to induce more uniform distribution of alloy elements. Then, the ingot of Φ120 mm was forged into the rods with Φ25 mm diameter at 1130 °C and cooled in air.

Thereafter, the experimental samples were cut from the forged rods, heated to 1020 °C for 1 h, and later quenched in water. Afterwards, the samples were heated to 640 °C for 2.5 h, followed by air cooling. According to GB/T 228–2015, the room temperature tensile tests were performed by using MTS CMT5205 testing machine with a strain rate of 0.00025 s^{-1} and 0.0067 s^{-1} before and after yielding, and high temperature tensile tests were conducted at 700 °C using MTS E45.105 testing machine with a strain rate of 0.00007 s^{-1}, 0.0014 s^{-1} before and after yielding. The tensile specimen with circular cross-section is machined into the dimension of total length of 90 mm, including the diameter of parallel part of 5 mm and the length of the parallel part of 30 mm [31].

The samples were manually and mechanically polished and etched by 4% nitric acid alcohol for microstructural observation. Scanning electron microscopy (SEM, Supra 55, Zeiss type) was employed to observe the morphology and distribution of structures and carbides. Moreover, the nano-carbides in samples were observed using the transmission electron microscopy (TEM, Titan ETEM, FEI) operating at 300 kV. TEM thin foils (diameter, 3 mm) were prepared by twin-jet electropolishing using the 5% perchloric acid alcohol solution. The Thermal-Calc software (TCFE6) was employed for the thermodynamic calculation of the effects of V on the formation of carbides.

Table 1
The nominal chemical compositions (wt%) of samples.

Elements Alloys with different contents of V	C	Ni	Cr	Mo	V	W	Nb	Fe
0% V	0.30	1.0	3.0	2.3	0	0.15	0.04	Bal.
0.4% V	–	–	–	–	0.4	–	–	Bal.
0.8% V	–	–	–	–	0.8	–	–	Bal.
1.2% V	–	–	–	–	1.2	–	–	Bal.

3. Results

3.1. Thermodynamic calculations

Fig. 1 a-d exhibits the variations in the equilibrium contents of $M_{23}C_6$, MC, M_2C and M_6C carbides respectively with the increase of V contents, by using the Thermal-Calc software. According to Fig. 1a, the mass fraction of $M_{23}C_6$ gradually decreases with the increasing temperatures. As the V content increases, the dissolution temperature of $M_{23}C_6$ decreases from 830 °C to 720 °C with the increase of V content, indicating that the stability of $M_{23}C_6$ decreases. Fig. 1b shows the effects of V content on the MC carbides. As observed from the figure, the content of MC increases to about 0.05% with an addition of 0.2% V. In the range of 0.2%–0.6%, the change of V content has little effect on the content of MC carbides. When the V content exceeds 0.6%, the mass fraction of MC carbides increases significantly, suggesting that the formation of MC carbide is strongly promoted with the V content from 0.6% to 1.2%. Fig. 1c displays the effects of V content on the formation of M_2C carbides. It is observed from the figure that V content has complicated effects on the M_2C carbides. To be specific, at the V content of less than 0.6%, the content of equilibrium M_2C carbides increases with the increase of V content, and the dissolution temperature of M_2C gradually increases. However, when the V content is higher than 0.6%, the influence of V is in the opposite direction. Fig. 1d shows that in the lower temperature region, the addition of V promotes the formation of equilibrium M_6C carbides, but in the higher temperature range, it shows a significant inhibitory effect on M_6C.

3.2. Tensile properties at room and elevated temperature

The tensile properties of samples with different V contents at room temperature are displayed in Fig. 2. Without the V addition, the ultimate tensile strength (UTS) and yield strength (YS) are determined to be 1125 MPa and 928 MPa, respectively. After the addition of 0.4% V, the UTS and YS of samples increase rapidly to 1315 MPa and 1165 MPa, respectively, accompanying with the elongation decreasing from 20% to 14%. The further increase in V content from 0.8% to 1.2%, the strength increases slowly from 1415 MPa to 1442 MPa, as well as the elongation decreases slightly from 14.1% to 12.2%.

Fig. 3 exhibits the UTS and YS of the samples with different V content at 700 °C. It can be seen from the figure that the UTS and YS are strongly dependent on the V content. With the content of V increasing from 0% to 0.4%, the UTS of the sample increases rapidly from about 395 MPa to 519 MPa and the YS increases from 282 MPa to 403 MPa. Besides, the increase rate in high temperature strength at 700 °C of the sample begins to slow down when the V content exceeds 0.4%, and the UTS of the 1.2% V sample is only about 30 MPa higher than that when the V content is 0.4% at 700 °C.

3.3. Microstructure observation

The microstructure observation on the samples with different V contents by SEM and TEM is presented in Fig. 4a–d. In Fig. 4a, the fine spherical intra-lath carbides and inter-lath strip-shaped carbides can be observed in 0% V sample. According to the bright-field TEM image of the lath in Fig. 4(a1), the width of the lath is about 0.5–1 μm. With the V content increase to 0.4%, the number of fine spherical carbides decreases and a large number of finer short rod-like carbides precipitate inside the lath, as shown in Fig. 4b. Meanwhile, the width of lath also decreases to 200–700 nm. With the further increase of V content to 0.8% and 1.2%, as shown in Fig. 4c and d, the length of rod-shaped carbides tends to shorten, and some larger spherical carbide precipitate along the lath boundaries. Compared with that of 0.4% V, the width of the laths with 0.8% V and 1.2% V changes slightly.

Fig. 5 exhibits the TEM morphology of rod-shaped carbides in the samples. It is obtained from the diffraction patterns that, they are all

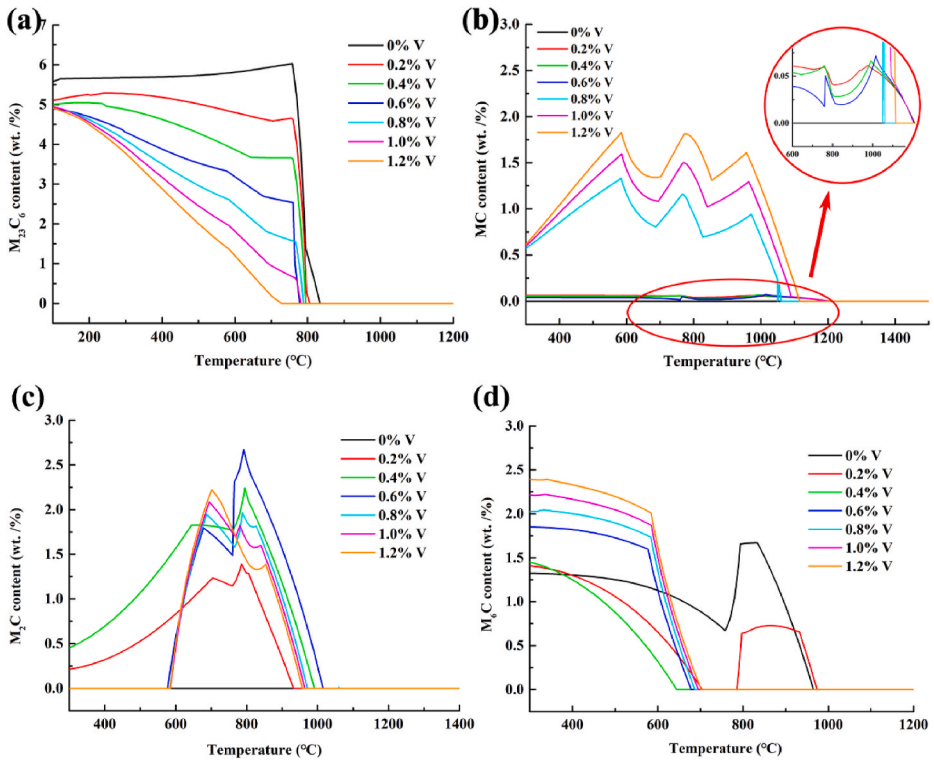

Fig. 1. Variations in carbide contents in the alloy with the increasing V content, (a) $M_{23}C_6$, (b) MC, (c) M_2C and (d) M_6C based on thermodynamic calculations of phase diagram.

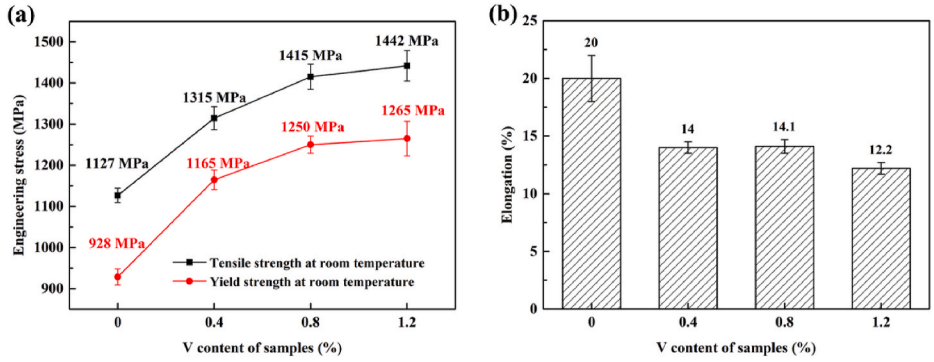

Fig. 2. Tensile properties of the samples quenched at 1020 °C and tempered at 640 °C, (a) tensile and yield strengths, and (b) elongation at room temperature.

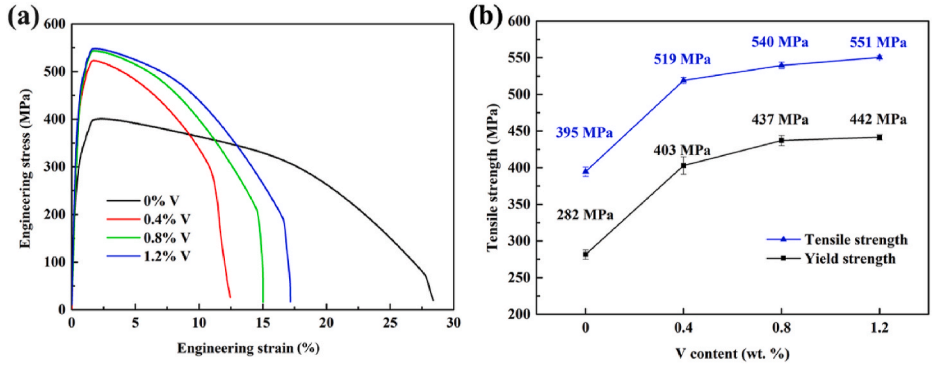

Fig. 3. Tensile properties of samples quenched at 1020 °C and tempered at 640 °C with different V content at 700 °C, (a) Stress-strain curves and (b) the variation of high-temperature strength.

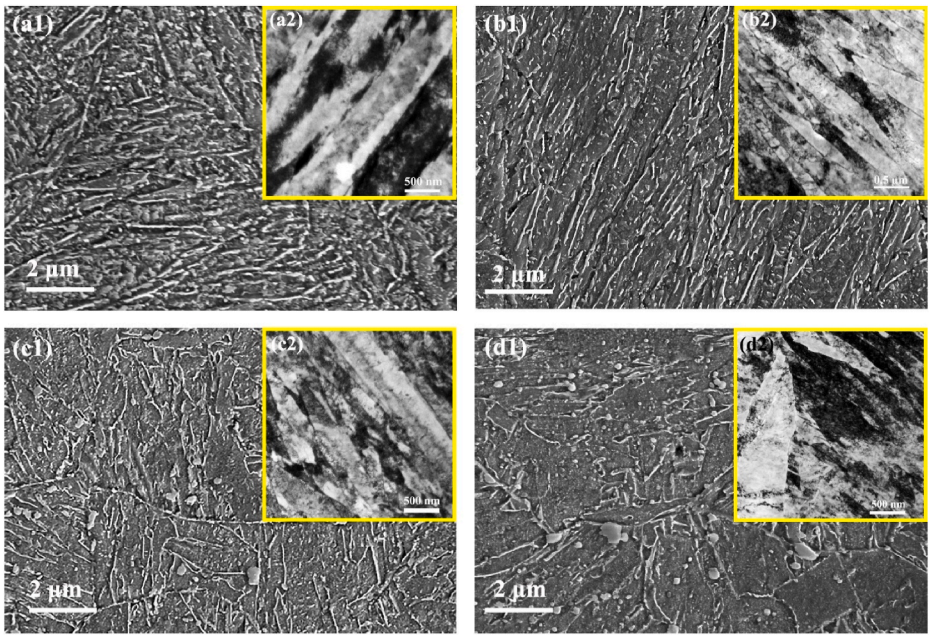

Fig. 4. The carbides and martensitic lath structure of samples quenched at 1020 °C and tempered at 640 °C, with different V contents of (a) 0% V, (b) 0.4% V, (c) 0.8% V, and (d) 1.2% V.

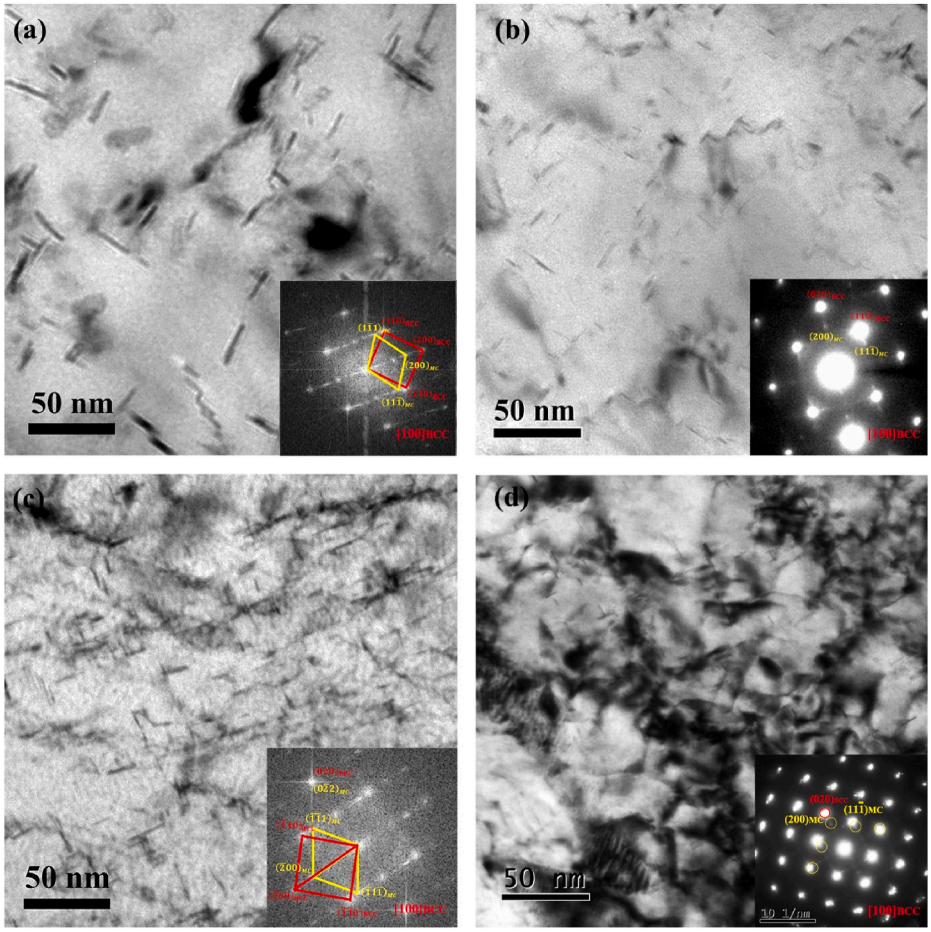

Fig. 5. The TEM micrographs containing nano-carbides in samples quenched at 1020 °C and tempered at 640 °C with different V contents of (a) 0% V, (b) 0.4% V, (c) 0.8% V, and (d) 1.2% V.

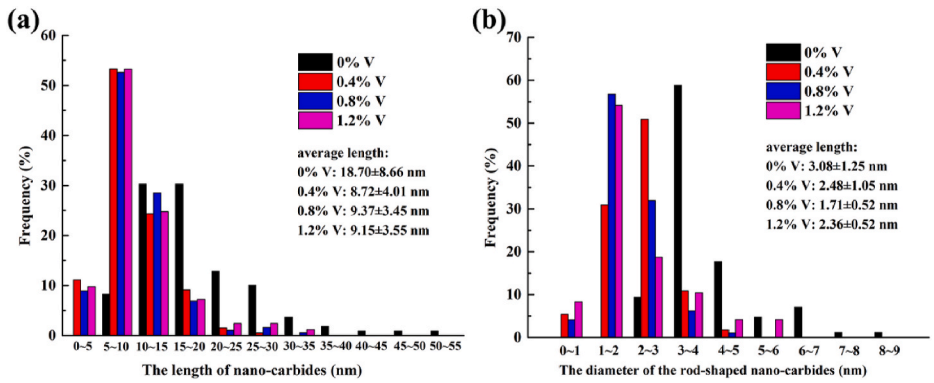

Fig. 6. The sizes of nano-carbides in samples quenched at 1020 °C and tempered at 640 °C with increasing V content, (a) the length, and (b) the cross-sectional diameter.

nano-scaled MC carbides, which follows a Baker-Nutting relationship [32] of $[010]_{MC}//[011]_{\alpha-Fe}$ and $(100)_{MC}//(100)_{\alpha-Fe}$. Fig. 6 shows the size distribution of MC nano-carbides in the samples with different V content. The average length and width of the nano-carbides is obtained by DM3 (DigitalMicrograph3) software. It can be seen that the average length of MC nano-carbides decreases greatly from 18.7 ± 8.66 nm to 8.72 ± 4.01 nm and the average cross-sectional diameter decreases from 3.08 ± 1.25 nm to 2.48 ± 1.05 nm after the addition of 0.4% V. With the further increase of V content from 0.4% to 1.2%, the size and length of MC carbide changes slightly.

The high resolution TEM (HRTEM) image of MC nano-carbides in 0% V and 0.8% V sample are shown in Fig. 7. The spacing of $(200)_{MC}$ of MC nano-carbides in 0% V and 0.8% V samples is determined to be 0.215 nm and 0.207 nm which can be identified as Nb-rich MC carbide and V-rich MC carbide respectively [33]. The lattice misfit (δ) of the V-free and 0.8% V samples are calculated to be 2.78% and 0.73% respectively by the formula [34] $\delta = \frac{(a_{carbide} - \sqrt{2}a_{\alpha Fe})}{a_{carbide}}$. The TEM morphology of samples with 0% V and 0.8% V after tensile test at 700 °C are presented in Fig. 8. As observed from Fig. 8a, the coarsened intra-crystalline carbides are found, which shows a high temperature tempering morphology of the martensite lath [35]. However, in the 0.8% V sample, the lath is well-defined, with no obvious coarsening carbides being detected inside or at the lath boundaries. In addition, nano-carbides with the length of 10–27 nm in the V-free sample are no longer visible in the TEM morphology, which are replaced by the rod-shaped carbides that are 100–200 nm in length (Fig. 8c), while a lot of nano-carbides are still observed in the 0.8% V sample. Moreover, results of selected area electron diffraction (SAED) pattern analysis show that, the secondary phases in Fig. 8a are identified to be M_2C with a HCP cubic structure [7, 36].

4. Discussions

The microstructural observation by SEM and TEM have shown that the addition of V has a strongly effect on the morphology and stability of MC nano-carbides. In tempered samples, the number of nano-carbides in V-containing samples is significantly higher, and finer and denser MC nano-carbides are observed in V-containing samples (Fig. 5). HRTEM images indicate that the lattice constant of MC nano-carbides decreases after the addition of V, which cause the reduction of the mismatch between the MC nano-carbide and the ferrite matrix. Moreover, after tensile test at 700 °C, it is observed that the rod-shaped MC nano-carbides in V-free sample disappears and is replaced by rod-shaped M_2C carbides with a larger size.

The refinement effect of V on the MC nano-carbides can be related to the increasing nucleation rate of the MC carbides in the V-containing samples. It has been reported that, the addition of V tends to form V clusters or V–C clusters in the initial stage of nucleation [37], which can provide more nucleus for MC nano-carbides. Apart from this, the V also has an effect on the elastic strain energy and interfacial energy. As shown in this study (Fig. 7), the addition of V leads to the reduction of interface misfit between MC nano-carbides and ferrite, which also facilitates the nucleation of nano-carbides by reducing the elastic strain energy during nucleation [38].

The increasing thermal stability of MC nano-carbides with the V

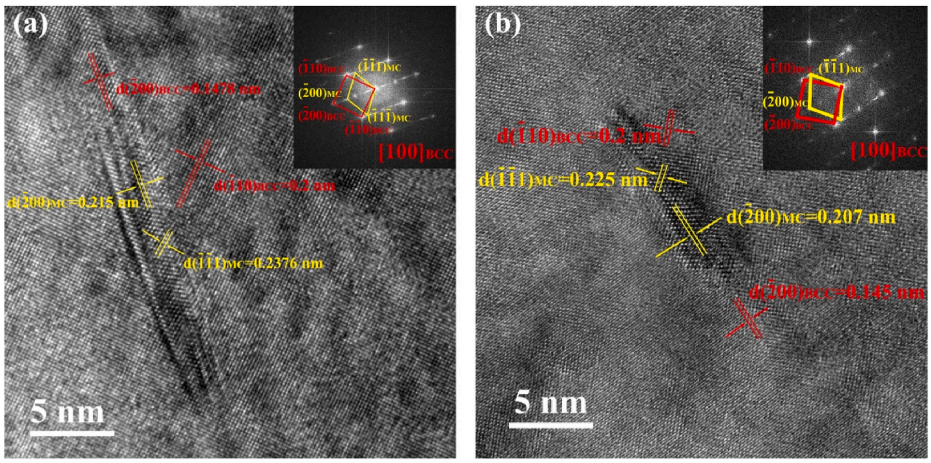

Fig. 7. HRTEM micrographs and the FFT pattern of nano-carbides in samples quenched at 1020 °C and tempered at 640 °C with different V contents of (a) 0% V sample, (b) 0.8% V sample.

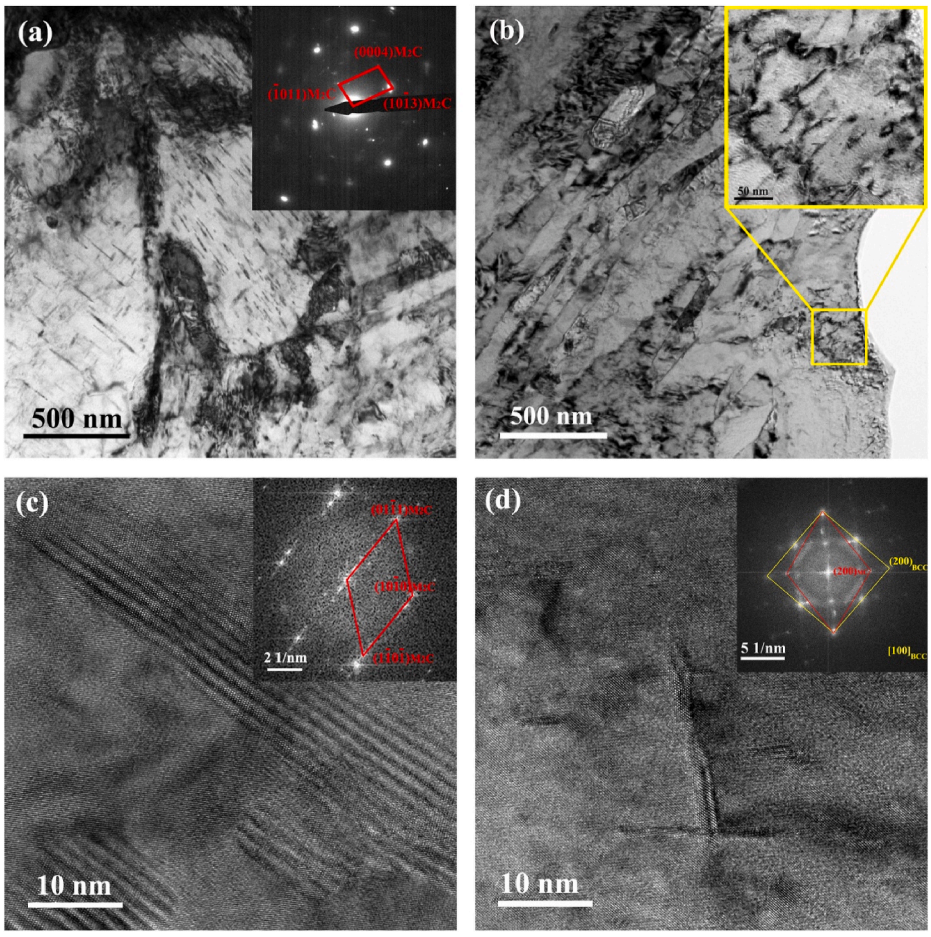

Fig. 8. Microstructure after high-temperature tensile test at 700 °C, TEM bright field images of (a) 0% V sample and (b) 0.8% V sample, and HRTEM micrographs of (c) M_2C in 0% V sample and (d) MC in 0.8% V sample.

addition during tempering can be related to the interfacial energy [38–41]. The larger lattice mismatch between Nb-rich MC nano-carbides and ferrite in the V-free samples can lead to a higher density of misfit dislocations and a higher interfacial energy compared with V-containing samples. Many simulation and calculation results [33, 40] also show that the interface energy of VC/α-Fe is lower than that of NbC/α-Fe, therefore the MC nano-carbides in V-free samples are easier to coarsen during high temperature tempering than the MC nano-carbides in V-containing samples.

With the increase of V content, the strength at room temperature and high temperature both increase significantly, as shown in Figs. 2 and 3. As a carbide forming element, it is reasonable to consider that the strengthening effect of V is mainly attributed to the carbide formation. The strengthening of carbides is achieved by hindering the movement of dislocations, which mainly includes two mechanisms, shearing and Orowan bypass mechanism. The improvement of yield strength based on shearing mechanism can be described as follow [42]:

$$\sigma_{Shearing} = \frac{2 \times 1.1}{\sqrt{2AG}} \times \frac{\gamma^{\frac{3}{2}}}{b^2} \times d^{\frac{1}{2}} f^{\frac{1}{2}} \tag{1}$$

Where G stands for the shear elasticity modulus, with the value of about 80.65 GPa; b is the absolute value of the Burgess vector of dislocation, which is about 0.248 nm; the interface energy γ of MC-type carbide is about 0.7 J m^{-2} [43]; d and f is the average diameter and the volume percentage of second-phase particle; A is the dislocation line tension function, which can be estimated by $A = \frac{1}{2\pi K} ln\left(\frac{d}{2b}\right)$. The value of K is related to the type of dislocation and Poisson's ratio ν of the material , K $= (1\text{-}\nu)$ is used for edge type dislocation, while K = 1 is adopted for screw dislocation, and for a mixed dislocation, the K can be estimated by $\frac{1}{K} = \frac{1}{2}\left(1 + \frac{1}{1-\nu}\right)$, Where ν is about 0.291 [44].

The improvement of yield strength based on the bypass mechanism can be described as the following equation [33]:

$$\sigma_{Orowan} = \frac{0.3728Gb}{K} \frac{f^{1/2}}{d} \ln\left(\frac{1.2d}{2b}\right) \tag{2}$$

Some views [39,45,46] hold that the shearing mechanism should be considered as leading mechanism due to the extremely small size of MC carbides and the coexistence with the matrix, whereas bypass mechanism should be adopted in other works [47]. In this study, the critical dimension (d_c) should be used to more accurately select the shearing mechanism or the bypass mechanism [42].

$$d_c = 0.209 \frac{Gb^2}{K\gamma} \ln\left(\frac{d_c}{2b}\right) \tag{3}$$

Where the value of G is about 80.65 GPa; b is 0.248 nm; γ is about 0.7 J m^{-2} [43]; After calculation, the d_c of nanoscale MC is determined to be about 2.2–4.7 nm, which is close to 3.5–5 nm in other reports [39,46].

The equivalent diameter calculation is adopted since the nano-carbides are rod-shaped or spindle-shaped [48]. The nano-carbides in the microstructure are assumed to be cylindrical, the equivalent diameter is calculated as the volume of spherical carbide, and the average value is calculated by $d_{ae} = \sqrt[3]{\frac{3}{2} l_a d_a^2}$, Where l_a is the average length and d_a represents the average diameter of the rod-shaped nano-carbides.

A statistical method is adopted to get the value of volume fraction of the second phase (f), it can be obtained by $f = \left(\frac{1.4\pi}{6}\right)\left(\frac{Nd_{ae}{}^2}{S}\right)$ [42]. Where, S represents the area of photos in nm^2, and N is the amounts of precipitates within a certain range.

The parameters related to the calculation of nano-carbides strengthening are listed in Table 2.

As shown in Table 2, the average equivalent size of the nano-carbides in the 0% V sample exceeds the critical size d_c, while those in other samples are mostly within the critical size. The calculation result of σ_{Orowan} for 0% V sample is about 257–362 MPa, which is consistent with other reports [18,49,50] exploring the bypass strengthening mechanism of nano-carbides. Meanwhile, the nano-carbides in 0.4%, 0.8% and 1.2% V samples contributed 516–613, 546–649, and 565–671 MPa, respectively. As shown in Fig. 9, the calculated yield strength increase caused by the nano-carbide is consistent with the variation of strength among the four samples obtained from room temperature tensile test, which shows a first rapid increase and then slow increase trend.

The V also has an effect on the high-temperature strength. As is shown in Fig. 3, with the increase of V content, the 700 °C strength increases from 400 MPa to 550 MPa, which is about 2 times higher than the universal used H13 steel as seen in Fig.S1. Due to the strength of both the ferrite matrix and the carbides will decrease with the temperature increases, and the steel matrix has a greater softening rate than the nano-carbides under high temperature conditions [51], therefore the dislocations will not easily cut through the carbides but be pinned and entangled around the carbides, as shown in Fig. 8. The pinning effect of carbides on dislocations is related to the volume fraction and the uniform dispersion of carbides [52]. As seen from the microstructure observation, the nano-carbides in V-containing samples are more stable during the high temperature tensile test. After high temperature tensile test at 700 °C, the 10–27 nm rod-shaped carbides in V-free samples are almost completely dissolved, and replaced by M_2C carbides with a size of about 100–200 nm, while the nano-carbides in the V-containing samples still exist stably (Fig. 8). Tao Wen et al. [21] discovered that, as V content increased from 0% to 0.14%, the size of rod-shaped carbides in the Fe–Cr–Ni–Mo steel gradually decreased, and a large amount of MC nano-carbides were observed, indicating that V contributed to stabilizing the MC nano-carbides and thus inhibiting the rapid generation of M_2C carbides. Therefore, the high-density intra-lath dislocations and MC nano-carbides that hinder the movement of dislocations under high temperature conditions should be the reasons for the increase in high-temperature strength [53–57].

5. Conclusions

This study investigates the effects of V contents from 0 to 1.2 wt% on the mechanical performances of MPS700V steel by thermodynamic calculations, mechanical performance testing and microstructure observation. The transformation of carbides, and the variations of their mechanical properties at room and high temperatures are discussed. The following conclusions are drawn from this work:

(1) With the increase of V content from 0 to 1.2% V, the ultimate tensile strength at room temperature increases from 1227 MPa to 1442 MPa, meanwhile the ultimate tensile strength at 700 °C increases from 400 MPa to 550 MPa ;
(2) Compared with sample without V, the MC nano-carbides in V-containing samples have a smaller size and more dispersed distribution. After the tensile test at 700 °C, the MC nano-carbides in 0.8% V containing sample shows high thermal stability while that in 0% V sample have transform to larger M_2C carbides. The addition of V reduces the interface misfit between MC nano-carbides and ferrite, which can be responsible for the high thermal stability of the carbides.

Table 2
The statistic results of nano-carbides parameters in the test alloys.

Parameters Alloys with different contents of V	l_a/nm	d_a/nm	d_{ae}/nm	f/%
0% V	18.7	3.077	6.428	0.65
0.4% V	8.7234	2.481	4.3186	1.10
0.8% V	9.375	1.713	4.474	1.21
1.2% V	9.145	2.361	4.244	1.32

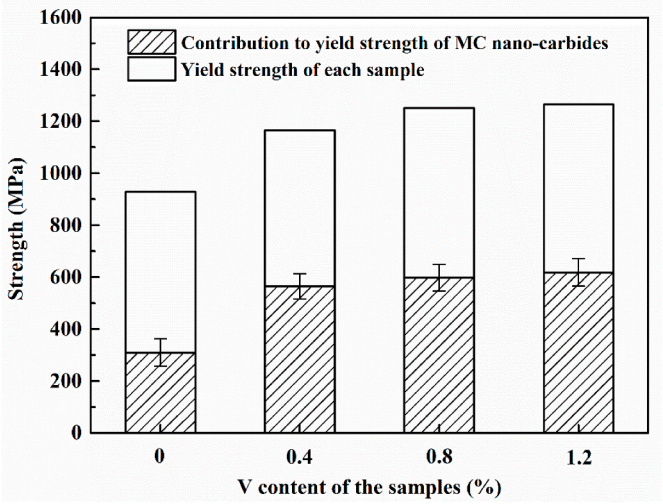

Fig. 9. Contribution to yield strength of the nano-carbides.

(3) The room temperature carbide strengthening mechanism transforms from the Orowan mechanism to the shear mechanism with the increasing content of V. At elevated temperature, the pinning effect of the stable and dispersed nano-scale MC carbide is observed in V-containing samples, which increases the high-temperature strength of the V-containing samples.

CRediT authorship contribution statement

Zunjun Zhang: Formal analysis, literature search, writing. **Jishan Zhang:** Design experiment. **Yong Lian:** Methodology. **Minyu Ma:** Fund management. **Chao Zhao:** Figures. **Huanyu Ye:** Operate TEM. **Gaojie Li:** Formal analysis. **Cheng Zhang:** Revision, language polishing, literature search. **Jinfeng Huang:** Design experiment, Funding acquisition.

Declaration of competing interest

We declare that we have no financial and personal relationships with other people or organizations that can inappropriately influence our work. This article has not been published elsewhere in whole or in part. All authors have read and approved the content, and agree to submit for consideration for publication in the journal. There are no any legal conflicts involved in the article.

Acknowledge

The authors are grateful to the Foundation of State Key Laboratory for Advanced Metals and Materials (2019Z-11).

Appendix A. Supplementary data

Supplementary data to this article can be found online at https://doi.org/10.1016/j.msea.2021.141091.

References

[1] Y.L. Wang, K.X. Song, Y.M. Zhang, G.X. Wang, Microstructure evolution and fracture mechanism of H13 steel during high temperature tensile deformation, Mater. Sci. Eng., A 746 (2019) 127–133.

[2] B. Wang, X. Zhao, W. Li, M. Qin, J. Gu, Effect of nitrided-layer microstructure control on wear behavior of AISI H13 hot work die steel, Appl. Surf. Sci. 431 (2018) 39–43.

[3] Y. Zhang, Y. Zhou, X. Guo, K. Song, X. Zhang, Fatigue failure prediction model and verification of hot extrusion die, Procedia Manufacturing 37 (2019) 66–72.

[4] Q. Zhou, X. Wu, N. Shi, J. Li, N. Min, Microstructure evolution and kinetic analysis of DM hot-work die steels during tempering, Mater. Sci. Eng., A 528 (2011) 5696–5700.

[5] D.H. Kim, H.C. Lee, B.M. Kim, K.H. Kim, Estimation of die service life against plastic deformation and wear during hot forging processes, J. Mater. Process. Technol. 166 (2005) 372–380.

[6] L. Shen, J. Zhou, X. Ma, X.Z. Lu, J.W. Tu, X. Shang, F. Gao, J.S. Zhang, Microstructure and mechanical properties of hot forging die manufactured by bimetal-layer surfacing technology, J. Mater. Process. Technol. 239 (2017) 147–159.

[7] A. Medvedeva, J. Bergström, S. Gunnarsson, J. Andersson, High-temperature properties and microstructural stability of hot-work tool steels, Mater. Sci. Eng., A 523 (2009) 39–46.

[8] J. Zhu, G.T. Lin, Z.H. Zhang, J.X. Xie, The martensitic crystallography and strengthening mechanisms of ultra-high strength rare earth H13 steel, Mater. Sci. Eng., A 797 (2020), 140139.

[9] Z. Jinxiang, H. Jinfeng, W. Hebin, L. Lin, C. Hua, Z. Jishan, Microstructures and mechanical properties of spray formed H13 tool steel, Acta Metall. Sin. 50 (2014) 787–794.

[10] W. Lee, S. Hong, C. Park, S. Park, Carbide precipitation and high-temperature strength of hot-rolled high-strength, low-alloy steels containing Nb and Mo, Metall. Mater. Trans. 33 (2002) 1689.

[11] R. Wan, F. Sun, L. Zhang, A. Shan, Development and study of high-strength low-Mo fire-resistant steel, Mater. Des. 36 (2012) 227–232.

[12] R. Uemori, R. Chijiiwa, H. Tamehiro, H. Morikawa, AP-FIM study on the effect of Mo addition on microstructure in Ti-Nb steel, Appl. Surf. Sci. 76–77 (1994) 255–260.

[13] W.B. Lee, S.G. Hong, C.G. Park, K.H. Kim, S.H. Park, Influence of Mo on precipitation hardening in hot rolled HSLA steels containing Nb, Scripta Mater. 43 (2000) 319–324.

[14] D. Zhao, L. Yong, L. Feng, Y. Wen, L. Zhang, Y. Dou, ODS ferritic steel engineered with bimodal grain size for high strength and ductility, Mater. Lett., 65 1672-1674.

[15] N. Mebarki, D. Delagnes, P. Lamesle, F. Delmas, C. Levaillant, Relationship between microstructure and mechanical properties of a 5% Cr tempered martensitic tool steel, Mater. Sci. Eng., A 387–389 (2004) 171–175.

[16] W. Dan, F. Wang, C. Jin, C. Li, Effects of Nb and tempering time on carbide precipitation behavior and mechanical properties of Cr-Mo-V steel for brake discs, Steel Res. Int. 89 (2018), 1700491.

[17] G.R. Speich, D.S. Dabkowski, L.F. Porter, Strength and toughness of Fe-10ni alloys containing C, Cr, Mo, and Co, Metallurgical Transactions 4 (1973) 303–315.

[18] I.B.T.A. Pereloma, Precipitate characterisation of an advanced high-strength low-alloy (HSLA) steel using atom probe tomography, Scripta Mater. 56 (2007) 601–604.

[19] D. Rojas, J. Garcia, O. Prat, G. Sauthoff, A.R. Kaysser-Pyzalla, 9%Cr heat resistant steels: alloy design, microstructure evolution and creep response at 650°C, Mater. Sci. Eng., A 528 (2011) 5164–5176.

[20] T. Siwecki, J. Eliasson, R. Lagneborg, B. Hutchinson, Vanadium microalloyed bainitic hot strip steels, ISIJ Int. 50 (2010) 760–767.

[21] T. Wen, X.F. Hu, Y.Y. Song, D.S. Yan, L.J. Rong, Carbides and mechanical properties in a Fe-Cr-Ni-Mo high-strength steel with different V contents, Mater. Sci. Eng., A 588 (2013) 201–207.

[22] Z. Wang, W. Hui, Z. Chen, Y. Zhang, X. Zhao, Effect of Vanadium on Microstructure and Mechanical Properties of Bainitic Forging Steel, Materials Science and Engineering: A, 2019, 138653.

[23] J.S.A. B, S.W.A. B, S.L.A. B, Influence of vanadium content on the precipitation evolution and mechanical properties of high-strength Fe–Cr–Ni–Mo weld metal, Mater. Sci. Eng., A 772 (2020), 138739.

[24] P. Michaud, D. Delagnes, P. Lamesle, M.H. Mathon, C. Levaillant, The effect of the addition of alloying elements on carbide precipitation and mechanical properties in 5% chromium martensitic steels, Acta Mater. 55 (2007) 4877–4889.

[25] H. Jo, C. Shin, J. Moon, J.H. Jang, H. Ha, S. Park, T. Lee, B.H. Lee, J. Chung, J. G. Speer, K.O. Findley, T.R. Jacobs, C. Lee, S. Kim, Mechanisms for improving tensile properties at elevated temperature in fire-resistant steel with Mo and Nb, Mater. Des. 194 (2020), 108882.

[26] N. Fujita, K. Ohmura, A. Yamamoto, Changes of microstructures and high temperature properties during high temperature service of Niobium added ferritic stainless steels, Mater. Sci. Eng., A 351 (2003) 272–281.

[27] Y.P. Song, X.M. Mao, W.Y. Wang, Z.Y. Ouyang, H.Y. Liang, L.L. Li, Effect of Re-Nb on the strength and toughness of 3Cr2MoNiWV cast hot working die steel, J. Mater. Sci. 41 (2006) 4185–4190.

[28] M. Ali, D. Porter, J. Kömi, M. Eissa, T. Mattar, The effect of double austenitization and quenching on the microstructure and mechanical properties of CrNiMoWMnV ultrahigh-strength steels after low-temperature tempering, Mater. Sci. Eng., A 763 (2019), 138169.

[29] K. Hrutkay, D. Kaoumi, Tensile deformation behavior of a nickel based superalloy at different temperatures, Mater. Sci. Eng., A 599 (2014) 196–203.

[30] M.A. Dangshen, J. Zhou, Z. Chen, Z. Zhang, Q. Chen, L.I. Dehui, Influence of thermal homogenization treatment on structure and impact toughness of H13 ESR steel, J. Iron Steel Res. Int. 16 (2009) 56–60.

[31] Z. Zhang, J. Zhang, Z. Yao, G. Xie, Y. Lian, M. Ma, C. Zhao, J. Huang, Design for novel hot-work die steel by thermodynamic calculation and microstructural examination, Metals-Basel 9 (2019) 805.

[32] R.G. Baker, Precipitation processes in steels, ISI Spec. Rep. 64 (1959) 1.

[33] Q. Yong, The Secondary Phase in Metal Material, Metallurgical Industry Press, 2006.

[34] C. Zhao, X. Xing, J. Guo, Z. Shi, Y. Zhou, X. Ren, Q. Yang, Micro-properties of (Nb, M) C carbide (M= V, Mo, W and Cr) and precipitation behavior of (Nb, V) C in carbide reinforced coating, J. Alloys Compd. 788 (2019) 852–860.

[35] G. Krauss, Tempering of lath martensite in low and medium carbon steels: assessment and challenges, Steel Res. Int. 88 (2017), 1700038.

[36] H.C. Wang, C. Somsen, Y.J. Li, S.G. Fries, E. Detemple, G. Eggeler, Effect of Nb on improving the impact toughness of Mo-containing low-alloyed steels, J. Mater. Sci. 54 (2019) 7307–7321.

[37] Q.D. Liu, W.Q. Liu, S.J. Zhao, Solute behavior in the initial nucleation of V- and Nb-containing carbide, Metall. Mater. Trans. 42 (2011) 3952–3960.

[38] J.H. Jang, C.H. Lee, Y.U. Heo, D.W. Suh, Stability of (Ti, M)C (M = Nb, V, Mo and W) carbide in steels using first-principles calculations, Acta Mater. 60 (2012) 208–217.

[39] Z. Xiong, I. Timokhina, E. Pereloma, Clustering, nano-scale precipitation and strengthening of steels, Prog. Mater. Sci. (2020), 100764.

[40] W.S. Jung, S.H. Chung, H.P. Ha, J.Y. Byun, An ab initio study of the energetics for interfaces between group V transition metal Nitrides and bcc iron, Model Simul. Mater. Sc. (2006) 14.

[41] Guo Zhanli, Sha Wei, Quantification of precipitation hardening and evolution of precipitates, Mater. Trans. 43 (2002) 1273–1282.

[42] J. Fu, G. Li, X. Mao, et al., Nanoscale cementite precipitates and comprehensive strengthening mechanism of steel, Metall. Mater. Trans. 42 (2011) 3797.

[43] Åsa Gustafson, Mats Hättestrand, Coarsening of precipitates in an advanced creep resistant 9% chromium steel—quantitative microscopy and simulations, Mater. Sci. Eng. 333 (2002) 279–286.

[44] A. Ning, M. Wenwen, C. Xichun, G. Hanjie, G. Jing, Precipitation behavior of carbides in H13 hot work die steel and its strengthening during tempering, Metals-Basel 7 (2017) 70.

[45] M. Charleux, W.J. Poole, M. Militzer, A. Deschamps, Precipitation behavior and its effect on strengthening of an HSLA-Nb/Ti steel, Metall. Mater. Trans. 32 (2001) 1635–1647.

[46] E. Pereloma, D. Cortie, N. Singh, G. Casillas, F. Niessen, Uncovering the mechanism of dislocation interaction with nanoscale (<4 nm) interphase precipitates in microalloyed ferritic steels, Materials Research Letters 8 (2020) 341–347.

[47] W.M. Rainforth, Effect of Nb-Mo additions on precipitation behaviour in V microalloyed TRIP-assisted steels, Metal Science Journal 32 (2016), 93491679.

[48] Q. Wang, C. Zhang, R. Li, J. Gao, M. Wang, F. Zhang, Characterization of the microstructures and mechanical properties of 25CrMo48V martensitic steel tempered at different times, Mater. Sci. Eng. 559 (2013) 130–134.

[49] F.Z. Bu, X.M. Wang, S.W. Yang, C.J. Shang, R.D.K. Misra, Contribution of interphase precipitation on yield strength in thermomechanically simulated Ti-Nb and Ti-Nb-Mo microalloyed steels, Mater. Sci. Eng., A 620 (2015) 22–29.

[50] J. Chen, M.Y. Lv, S. Tang, Z.Y. Liu, G.D. Wang, Influence of cooling paths on microstructural characteristics and precipitation behaviors in a low carbon V-Ti microalloyed steel, Mater. Sci. Eng., A 594 (2014) 389–393.

[51] W. Li, J. Ma, H. Kou, J. Shao, X. Zhang, Y. Deng, Y. Tao, D. Fang, Modeling the effect of temperature on the yield strength of precipitation strengthening Ni-base superalloys, Int. J. Plast. 116 (2019) 143–158.

[52] Z. Wang, H. Zhao, L. Chen, G. Wu, M. Wang, Evolution and its stability of $M_{23}(C, N)_6$ carbonitride in martensite ferritic steel during long-term thermal aging, Mater. Char. 152 (2019) 36–43.

[53] K. Miyata, T. Kushida, T. Omura, Y. Komizo, Coarsening kinetics of multicomponent MC-type carbides in high-strength low-alloy steels, Metall. Mater. Trans. 34 (2003) 1565–1573.

[54] J. Takahashi, K. Kawakami, J. Hamada, K. Kimura, Direct observation of niobium segregation to dislocations in steel, Acta Mater., 107 415-422.

[55] S.L. Shrestha, K.Y. Xie, S.P. Ringer, K.R. Carpenter, D.R. Smith, C.R. Killmore, J. M. Cairney, The effect of clustering on the mobility of dislocations during aging in Nb-microalloyed strip cast steels: in situ heating TEM observations, Scripta Mater. 69 (2013) 481–484.

[56] Z.M. Shi, W. Gong, Y. Tomota, S. Harjo, J. Li, B. Chi, J. Pu, Study of tempering behavior of lath martensite using in situ neutron diffraction, Mater. Char. 107 (2015) 29–32.

[57] Y. Peng, L. Yu, Y. Liu, Z. Ma, H. Li, C. Liu, J. Wu, Microstructures and tensile properties of an austenitic ODS heat resistance steel, Mater. Sci. Eng., A 767 (2019), 138419.